



HAL
open science

KINETICS OF METHANOL DECOMPOSITION OF Rh(100) AND Rh(111) FIELD EMITTERS

G. Chuah, N. Kruse, J. Block, G. Abend

► **To cite this version:**

G. Chuah, N. Kruse, J. Block, G. Abend. KINETICS OF METHANOL DECOMPOSITION OF Rh(100) AND Rh(111) FIELD EMITTERS. Journal de Physique Colloques, 1988, 49 (C6), pp.C6-215-C6-220. 10.1051/jphyscol:1988636 . jpa-00228133

HAL Id: jpa-00228133

<https://hal.science/jpa-00228133>

Submitted on 4 Feb 2008

HAL is a multi-disciplinary open access archive for the deposit and dissemination of scientific research documents, whether they are published or not. The documents may come from teaching and research institutions in France or abroad, or from public or private research centers.

L'archive ouverte pluridisciplinaire **HAL**, est destinée au dépôt et à la diffusion de documents scientifiques de niveau recherche, publiés ou non, émanant des établissements d'enseignement et de recherche français ou étrangers, des laboratoires publics ou privés.

KINETICS OF METHANOL DECOMPOSITION OF Rh(100) AND Rh(111) FIELD EMITTERS

G.K. CHUAH, N. KRUSE*, J.H. BLOCK* and G. ABEND*

Department of Chemistry, National University of Singapore, Singapore
**Fritz-Haber-Institut der Max-Planck-Gesellschaft, Faradayweg 4-6,*
D-1000 Berlin 33, F.R.G.

Abstract – The decomposition of methanol on Rh has been investigated by means of pulsed field desorption mass spectrometry (PFDMS). Intermediates of the decomposition, CH_xO ($x = 1 - 3$), are identified. By varying the temperature and reaction time it is possible to elucidate the elementary steps in methanol decomposition. A model based on a stepwise H-abstraction of the methoxy is postulated. The reaction becomes desorption-rate limited if the final products, $\text{CO}_{(\text{ad})}$ and $\text{H}_{(\text{ad})}$, are not removed from the surface and block sites required for reaction. However, by using a desorption field high enough to quantitatively remove the final products, the rate-determining step is found to be the removal of the H from the methoxy. Computer simulations support this observation.

I. Introduction

Methanol is of considerable economic value both as a feedstock for the production of other chemicals and as a source of fuel.¹ Since supported transition metal catalysts have been found to be active in methanol synthesis, an understanding of the reaction mechanism is important. Surface techniques usually require high vacuum conditions. They are therefore not suitable to study the methanol synthesis from CO and H_2 . Instead, the decomposition of methanol has been examined, because it is expected that the same intermediates will be found in the decomposition as in the synthesis reaction. Methanol decomposition has been investigated on metals such as Ni^{2-5} , Pd^{6-8} , $\text{Fe}^{9,10}$, $\text{Pt}^{11,12}$ and Ru^{13-15} . A methoxy species formed at the surface of the transition metals is stable only below room temperature. On rhodium¹⁶, the methoxy decomposes around 200 K and carbon monoxide and hydrogen are formed as the final products. No other intermediates have been identified. In the present study, pulsed field desorption mass spectrometry (PFDMS) is employed to follow the kinetics of methanol decomposition as a function of temperature and coverage. With a time resolution better than 100 μs , this technique offers the opportunity to detect short-lived intermediates.

II. Experimental

The detailed setup of PFDMS has been previously reported¹⁷. High voltage pulses are used to remove the adsorbed layer from a field emitter tip. The desorbing ions are identified by time-of-flight mass spectrometry. The field pulses can have amplitudes up to 20 kV, repetition frequency ≤ 10 kHz, and half-widths of ≈ 100 ns.

Experiments are performed with continuous flow of the gas. In the time interval between pulses, t_R , molecules impinge on the tip, adsorb and undergo reaction. The next pulse desorbs the adlayer and reactants, intermediates and products can be identified. The total desorption field strength, F_D , is the sum of the field pulse, F_P , and a steady field, F_R , which may be applied during t_R . The influence of the field pulse on the reaction is considered to be negligible because of its short duration (≈ 100 ns) as compared to the much longer reaction time, $t_R \geq 100 \mu\text{s}$. However, a steady field, F_R , can be applied in order to investigate the influence of the electrical field on the surface processes.

Rhodium emitters were prepared from wires (Goodfellows, 0.1 mm ϕ) by etching in molten $\text{NaCl}/\text{NaNO}_3$ (1:4 w/w). The tips were subsequently cleaned by combined cycles of heating and field evaporation. Surface temperatures are measured by a Chromel-Alumel thermocouple spotwelded onto the shank of the tip. CH_3OH (E. Merck, p.a. grade) and methyl- d_2 alcohol – CHD_2OH (MSD Isotopes, 98.6 atom% D) were freed from dissolved gases by several freeze-pump-thaw cycles before dosing.

III. Results

The decomposition of methanol on Rh(100)- and Rh(111)-oriented emitters was studied. Fig. 1a shows a typical mass scan of the desorbing ions. In the absence of a steady electrical field between pulses, the main species detected are the final products of methanol decomposition, CO^+ and H_n^+ , as well as smaller intensities of CH_3^+ and H_yO^+ ($y = 0 - 3$). The presence of CH_3^+ ions is attributed to C-O bond cleavage in the adsorbed methoxy¹⁸. This seems to be preferred over O-Rh bond breaking which results in CH_3O^+ ions. A steady field $F_R \geq 4$ V/nm increases the concentration of certain intermediates at the surface. Fig. 1b shows a mass spectrum taken with methyl- d_2 alcohol, CHD_2OH . Here, the main species detected are the deuterated analogues of CH_3^+ , CH_2O and the protonated parent molecule. The effect of an electrical field to slow down the methanol decomposition reaction by stabilizing the the intermediates has been reported previously¹⁸.

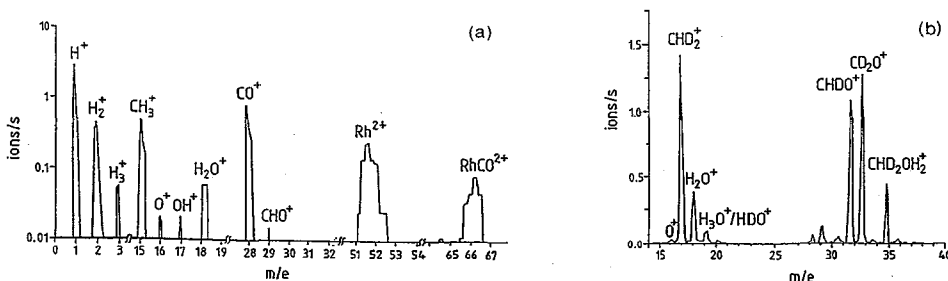


Figure 1 Mass spectrum of field desorbed ions from a rhodium tip using
 (a) CH_3OH , $F_R = 0$ V/nm, $F_D \approx 28$ V/nm, $t_R = 1$ ms, $T = 298$ K, $p = 1.3 \times 10^{-5}$ Pa.
 (b) CHD_2OH in the presence of a steady electric field,
 $F_R = 4$ V/nm, $F_D = 28$ V/nm, $t_R = 0.2$ ms, $T = 298$ K, $p = 1.3 \times 10^{-5}$ Pa.

III.1. Temperature Variation

More insight into the path of methanol decomposition is gained by studying the temperature dependence of the reactions. Fig. 2 shows the results of measurements using CH_3OH ($p = 1.3 \times 10^{-5}$ Pa) in the presence of a steady electric field, $F_R = 3$ V/nm. The total desorption field strength was approximately 27 V/nm.

At low temperatures, high intensities of CH_3^+ , CH_2O^+ and H_yO^+ are detected. However, only small intensities of H_n^+ , CO^+ and $\text{Rh}(\text{CO})^{2+}$ are observed. The rather high intensity of intermediates is due to field stabilization. Above 320 K, the CH_2O^+ ion rate decreases rapidly. Coinciding with this drop is a sharp rise in the intensities of H_n^+ and CO^+ . This indicates an acceleration of the forward reaction which counteracts the field-stabilization of CH_2O . It also proves that CH_2O is an intermediate in the reaction as by its decomposition, higher intensities of the final products, CO and H, are observed. CH_2O^+ appears to be very sensitive to temperature whereas the CH_3^+ ion rate remains high up to ≈ 430 K. Above this temperature, its intensity falls rapidly. The decrease in the CH_3^+ ion rate above 430 K indicates that here the enhancement in reaction rate due to the higher temperatures can no longer be balanced by field stabilization.

The H_n^+ signal shows a maximum at about 380 K and decreases with higher temperatures. Since thermal desorption of hydrogen¹⁹ occurs at 380 K, the surface coverage of hydrogen drops with temperature. Consequently, the H_n^+ intensity decreases at temperatures above 380 K. The intensities of CO^+ and $\text{Rh}(\text{CO})^{2+}$ have been summed together in Fig. 2 as the field pulses may desorb $\text{CO}_{(\text{ad})}$ as either CO^+ or with the simultaneous removal of a Rh atom. The combined intensities of CO^+ and $\text{Rh}(\text{CO})^{2+}$ remain high up to ≈ 500 K. Above this temperature, the ion rate falls. This is in agreement with thermal desorption spectroscopy which shows that carbon monoxide desorbs at 528 K from the Rh(100) surface²⁰.

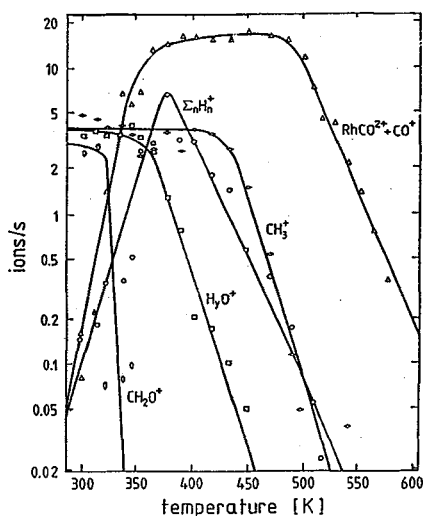


Figure 2 Dependence of the ion intensities with temperature in the presence of a steady electric field. CH_3OH : 1.3×10^{-5} Pa, $t_R = 200 \mu\text{s}$, $F_P = 24$ V/nm, $F_R \approx 3$ V/nm, $F_D = 27$ V/nm.

The H_3O^+ species peaks at 340 K and decreases steadily with higher temperatures. The high intensity of H_3O^+ may be due to the steady electric field which increases the binding energy of the water molecule to the metal surface. Additionally, inhomogeneities at the tip surface generate local high field regions when a continuous voltage is applied. Diffusion of water into these areas may thus be enhanced and account for the high H_3O^+ signal. Above 340 K, the effect of field enhancement is offset by the shorter residence time of water molecules at the surface. Hence, the H_3O^+ rate decreases.

III.2. Variation of Reaction Time

Information on the reaction rates can be obtained by monitoring the surface concentration of the various species involved in the catalytic reaction. Unfortunately, under field-free conditions, the low concentrations of intermediates other than the methoxy made elucidation of the kinetics meaningless because of large statistical error. Hence, a steady electrical field was applied during the measurements in order to stabilize the intermediates, especially CH_2O , and to sufficiently slow down the reaction to within the range of the method.

Fig. 3 shows the results of varying the reaction time. A steady electrical field of about 5 V/nm was applied during these measurements. The rhodium field emitter was kept at room temperature and dosed with methyl- d_2 alcohol, CHD_2OH , at $p = 1.3 \times 10^{-5}$ Pa. The surface concentrations (measured as ions/pulse) of the respective species built up in the reaction time t_R are plotted as a function of t_R . Different time dependencies are exhibited by the various ions. For $100 \mu\text{s} < t_R < 5$ ms, CHD_2^+ and "deuterated formaldehyde" — CHDO^+ , CD_2O^+ — dominate the mass spectra. The intensity of the "deuterated formaldehyde" is lower than CHD_2^+ . Both species increase linearly with the reaction time. At $t_R \approx 1$ ms, CO^+ appears. The initial slope of the CO^+ curve indicates a quadratic dependence with time.

The $\text{H}_x\text{D}_y\text{O}^+$ ($x, y = 0 - 3$) signal increases linearly at short reaction times but levels out at $t_R > 1$ ms. This final level is due to thermal desorption of water which limits the surface concentration at long reaction times.

For the decomposition of CHD_2O , a kinetic isotope effect is observed²¹. The measured intensity of CD_2O^+ is approximately equal to CHDO^+ (Fig. 1b), showing that the breaking of a C-H bond in CHD_2O is twice as facile as a C-D bond cleavage. In the absence of any isotope effect, the intensity of CHDO^+

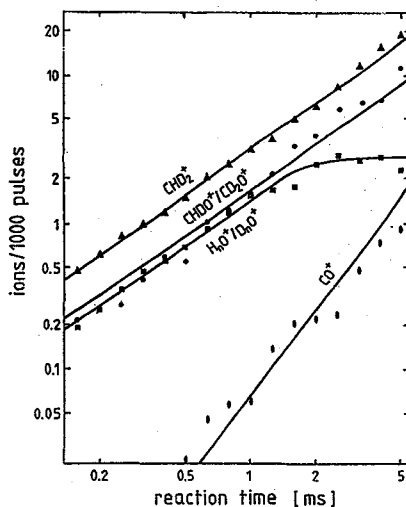


Figure 3 Dependence of the ion intensities with reaction time.

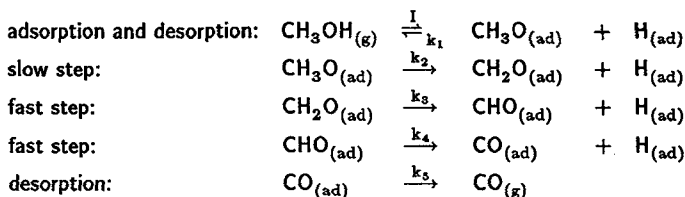
$F_P = 23$ V/nm, $F_R = 5$ V/nm, $F_D = 28$ V/nm, $T = 298$ K, $p = 1.3 \times 10^{-6}$ Pa.

should be twice that of CD_2O^+ according to the statistical ratio of D to H in the CHD_2O species.

IV. Discussion

The presence of a field stabilizes both CH_2O and CH_3O (as indicated by the CH_3^+ signal). The extent of stabilization depends on the interaction of the individual species with the electrical field and can be counteracted by applying a higher temperature. Hence, it is seen from Fig. 2 that the CH_2O^+ intensity decreases already at 320 K while the CH_3^+ ion rate remains high up to 430 K. It is clear that CH_2O is an intermediate in the decomposition reaction as the decrease in its ionic intensity at 320 K coincides with an increased ionic rate of the final products, CO^+ and H_n^+ . The detection of only CH_3^+ and CO^+ ions at high temperatures shows that the decomposition of the methoxy species is slow while the subsequent steps are fast. However, the overall rate of reaction is limited by thermal desorption of the final product, adsorbed carbon monoxide. Only at temperatures above ≈ 500 K does the $CO_{(ad)}$ thermally desorb. Below this temperature, its formation inhibits the steady methanol decomposition. This inhibition can be removed under the conditions of PFDMS experiments by applying high field pulses to desorb the $CO_{(ad)}$ immediately after its formation. Quantitative desorption of CO is certainly the case at high pulse repetition frequencies.

Kinetic information is gained from an analysis of the plots showing ion count rates versus reaction time. Considering a simple model for dissociative adsorption, desorption and forward reaction via intermediates, the following equations can be written:



As the reaction time variation experiments involve only low coverages of methanol, ($p = 1.3 \times 10^{-6}$ Pa, $100 \mu s < t_R < 5$ ms), blocking of sites is not considered in the above model. A numerical analysis for the above equations was performed. With the used set of rate constants (Fig. 4), the methoxy and the

CH_2O increase linearly with time whereas the carbon monoxide concentration initially shows a quadratic time dependence. The quadratic time dependence of the final product only occurs if $k_3:k_2 > 100$. At longer times, the quadratic dependence changes over to a linear dependence. The pressure used in this computation is 1.3×10^{-5} Pa so that a monolayer coverage would be attained only after 10 s. Therefore, saturation of the surface and consequently blocking of the reaction is not observed.

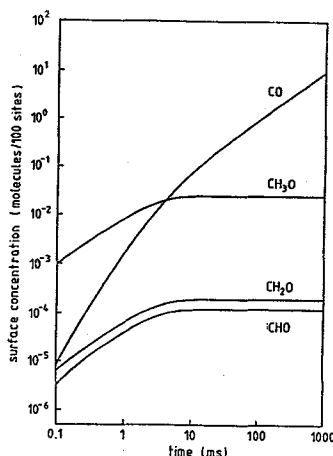


Figure 4 Numerically calculated curve when there is no blocking of sites.

Rate constants: $k_1 = 10 \text{ s}^{-1}$, $k_2 = 400 \text{ s}^{-1}$, $k_3 = 50000 \text{ s}^{-1}$, $k_4 = 80000 \text{ s}^{-1}$, $k_5 = 0 \text{ s}^{-1}$.

Pressure = 1.3×10^{-5} Pa, number of sites = 100.

The calculated curves fit quite well with the experimental results (Fig. 3) for $100 \mu\text{s} < t_R < 5 \text{ ms}$. The intensity of CHD_2^+ increases linearly with time. This fits with the proposed model where the methoxy is a function of impingement rate and reaction time. The "deuterated formaldehyde" curve also shows a first-order dependence with time. Its concentration is higher than predicted from the model and this is due to field stabilization. The CO^+ curve grows initially with a second-order dependence on the reaction time. Hence, it can be concluded from a comparison of the experimental results with the model that the slow step in steady methanol decomposition has to be the hydrogen abstraction in the methoxy. This conclusion is further supported by the high CH_3^+ intensities detected at temperatures below 430 K (Fig. 2) and the observation of a deuterium kinetic isotope effect in the formation of the "deuterated formaldehyde".

However, at times longer than 5 ms (not shown in Fig. 3), the experimental curves deviate from the expected pattern. Their behaviour suggest a poisoning of the surface which occurs already at relatively low coverage. Future work is necessary to determine the mechanism of this poisoning. On Ni(111) crystal, Gates et al.^{4,5} observed that the final products of methanol decomposition, $\text{CO}_{(\text{ad})}$ and $\text{H}_{(\text{ad})}$, inhibit the reaction. Richter and Ho²² also proposed a site blocking model for methanol decomposition on Ni(110) where desorption of hydrogen is coupled to the reaction channel. In our measurements with PFDMS, the field-induced cleavage of the $\text{CH}_3\text{O}_{(\text{ad})}$ results in surface O which can react with the $\text{H}_{(\text{ad})}$ to form water. This provides an effective route for the removal of $\text{H}_{(\text{ad})}$ and thus, $\text{H}_{(\text{ad})}$ is not expected to have a severe inhibition effect as $\text{CO}_{(\text{ad})}$ which is more strongly bonded to the metal. Furthermore, high desorption field pulses are normally used to remove $\text{CO}_{(\text{ad})}$ and $\text{H}_{(\text{ad})}$, thus allowing steady decomposition of methanol to proceed. At very fast pulse repetition frequencies, the $\text{CO}_{(\text{ad})}$ and $\text{H}_{(\text{ad})}$ are efficiently desorbed and do not accumulate at the surface. However, at long times (low pulse frequencies), the adsorbed products may accumulate and block sites for adsorption and reaction. This may account for the poisoning we observed at long times ($t_R \geq 5 \text{ ms}$).

V. Conclusion

Our results point to a mechanism involving dissociative adsorption of methanol followed by stepwise hydrogen abstraction from the resulting methoxy. This is corroborated by the detection of the intermediates, CH_xO ($x = 1 - 3$). The detection of high intensities of the methoxy under steady-state conditions and up to high temperatures indicates that the rate-determining step is the C-H bond breaking to form CH_2O species. The rate constant in this step is numerically calculated to be at least 100-times smaller than the rate constants in the subsequent reactions leading to CO and H.

Acknowledgement

One of us (GKC) wants to thank the National University of Singapore for financial support.

References

- (1) Wender, I. *Catal. Rev. - Sci. Eng.* **1984**, *26*, 303.
- (2) Demuth, J. E.; Ibach, H. *Chem. Phys. Lett.* **1979**, *60*, 395.
- (3) Erskine, J. L.; Bradshaw, A. M. *Chem. Phys. Lett.* **1980**, *72*, 260.
- (4) Gates, S. M.; Russell, J. N., Jr.; Yates, J. T., Jr. *Surface Sci.* **1984**, *146*, 199.
- (5) Gates, S. M.; Russell, J. N., Jr.; Yates, J. T., Jr. *J. Catal.* **1985**, *92*, 25.
- (6) Kok, G. A.; Noordermeer, A.; Nieuwenhuys, B. E. *Surface Sci.*, **1983**, *135*, 65.
- (7) Christmann, K.; Demuth, J. E. *J. Chem. Phys.* **1982**, *76*, 6308.
- (8) Christmann, K.; Demuth, J. E. *J. Chem. Phys.* **1982**, *76*, 6318.
- (9) Benziger, J. B.; Madix, R. J. *J. Catal.* **1980**, *65*, 36.
- (10) McBreen, P. H.; Erley, W.; Ibach, H. *Surface Sci.* **1983**, *133*, L469.
- (11) Sexton, B. A. *Surface Sci.* **1981**, *102*, 271.
- (12) Ehlers, D. H.; Spitzer, A.; Lüth, H. *Surface Sci.* **1985**, *160*, 57.
- (13) Goodman, D. W.; Yates, J. T., Jr.; Madey, T. E. *Chem. Phys. Lett.* **1978**, *53*, 479.
- (14) Hrbek, J.; dePaola, R. A.; Hoffmann, F. M. *J. Vac. Sci. Technol.* **1983**, *A1*, 1222.
- (15) Hrbek, J.; dePaola, R. A.; Hoffmann, F. M. *J. Chem. Phys.* **1984**, *81*, 2818.
- (16) Solymosi, F.; Berkó, A.; Tarnóczy, T. I. *Surface Sci.* **1984**, *141*, 533.
- (17) Block, J. H.; Czanderna, A. W. In *Methods of Surface Analysis*; Czanderna, A. W., Ed.; Methods and Phenomena I: Their Applications in Science and Technology; Elsevier: Amsterdam, 1975; Vol. 1, p 379.
- (18) Kruse, N.; Chuah, G.-K.; Abend, G.; Cocke, D. L.; Block, J. H. *Surface Sci.* **1987**, *189/190*, 832.
- (19) Yates, J. T., Jr.; Thiel, P. A.; Weinberg, W. H. *Surface Sci.* **1979**, *84*, 427.
- (20) Castner, D. G.; Sexton, B. A.; Somorjai, G. A. *Surface Sci.* **1978**, *71*, 519.
- (21) Chuah, G.-K.; Kruse, N.; Schmidt, W. A.; Abend, G.; Block, J. H., to be published.
- (22) Richter, L. J.; Ho, W. *J. Chem. Phys.* **1985**, *83*, 2569.